Asian Journal of Andrology (2022) 24, 207–212
www.asiaandro.com; www.ajandrology.com

Open Access

ORIGINAL ARTICLE

Sexual Function

Experimental investigation of early assessment of corpora cavernosa fibrosis with two-dimensional shear wave elastography

Li Yu[1,*], Wan-Ting Rao[2,*], Jing-Dong Tang[3], Jin-Fang Xing[2,3]

This study explored the usefulness of two-dimensional shear wave elastography (2D-SWE) in the early assessment of corpora cavernosa fibrosis (CCF). New Zealand male rabbits were randomly assigned to an experimental group or a control group. Recombinant human transforming growth factor beta 1 (TGF-β1) was injected into the dorsal penis tissue of rabbits in the experimental group. Conventional ultrasound and 2D-SWE examinations were performed before and 20 days after injection. Penile histological analysis was performed by hematoxylin–eosin staining, sirius red staining, and immunohistochemistry. Measurement of 2D-SWE examination results was performed using shear wave elastography quantitative measurement (SWQ). Histological analysis outcomes were the proportion of smooth muscle cells (SMCs), collagen fibers (CFs), collagen type I (Col I), and collagen type III (Col III), as well as the SMCs/CFs ratio, measured by sirius red staining. Other histological analysis outcomes were the positive area proportion (PAP) of TGF-β1 (PAP_T), fibronectin (PAP_F), and Col III (PAP_C), measured by immunohistochemistry. After recombinant human TGF-β1 injection, SWQ was higher in the experimental group than that in the control group ($P < 0.001$); however, there were no differences in conventional ultrasound results. There were significant differences in histological outcomes between the two groups (all $P < 0.05$). These results indicated that 2D-SWE was superior for identifying early histological changes in CCF.

Asian Journal of Andrology (2022) **24**, 207–212; doi: 10.4103/aja202147; published online: 03 September 2021

Keywords: collagen type I; collagen type III; elastography; penis; smooth muscle cells

INTRODUCTION

Corpora cavernosa fibrosis (CCF) is a common andrological condition, which is characterized by fibrous cord or plaque in the corpora cavernosa.[1,2] At present, the diagnosis of CCF mainly depends on medical history, physical examination, and imaging modalities that are used to identify the characteristics, location, size, and calcification of the cord or plaque.[3] Currently, the most important diagnostic characteristic for CCF is the detection of the cord or plaque, but there is usually no effective treatment that targets the cord or plaque.

Before cord or plaque formation, the local tissue components (*e.g.*, cells and extracellular matrix [ECM]) exhibit substantial changes, primarily in terms of inflammatory cell recruitment, fibroblasts proliferation, collagen fibers (CFs) accumulation, and smooth muscle cells (SMCs)/CFs imbalance.[1,2,4] If the diagnosis of CCF could be made at this stage and followed by effective antifibrotic treatment, it would greatly help alleviate symptoms, shorten the disease course, and achieve a favorable prognosis.

Two-dimensional shear wave elastography (2D-SWE) is a new ultrasound elastography technique that can quantitatively analyze changes in tissue composition.[5–7] Because local tissue components in the penis usually change before cord or plaque formation, early diagnosis of CCF can be achieved with the application of 2D-SWE by detecting histological changes in penile tissue. This study aimed to analyze changes in penile tissue components before cord or plaque formation; it also aimed to perform 2D-SWE imaging on the penis and obtain shear wave elastography quantitative measurement (SWQ) values. Finally, this study explored the usefulness of 2D-SWE in the early diagnosis (*i.e.*, before cord or plaque formation) of CCF.

MATERIALS AND METHODS

Experimental animals

Twenty New Zealand male rabbits (4–5 months of age) were randomly assigned to an experimental (transforming growth factor beta 1 [TGF-β1]) group and a control group ($n = 10$ for each group). Rabbits in the TGF-β1 group had a body weight (mean ± standard deviation [s.d.]) of 2.53 ± 0.20 (range: 2.20–2.85) kg, and rabbits in the control group had a body weight (mean ± s.d.) of 2.51 ± 0.29 (range: 2.10–3.00) kg. Both groups of rabbits were kept in the same environment (*i.e.*, same room temperature and diet) and were acclimated for 1 week. This study protocol was approved by the Ethics Committee of Fudan University Pudong Medical Center, Shanghai, China ([2018] No. [WZ-13]).

[1]Department of Special Inspection, Shanghai Shibei Hospital of Jing'an District, Shanghai 200435, China; [2]Department of Medical Ultrasound, Fudan University Pudong Medical Center, Shanghai 201399, China; [3]Shanghai Key Laboratory of Vascular Lesions Regulation and Remodeling, Fudan University Pudong Medical Center, Shanghai 201399, China.
Correspondence: Dr. JF Xing (xingshi70188@163.com)
*These authors contributed equally to this work.
Received: 05 January 2021; Accepted: 22 June 2021

CCF modeling

The CCF model was constructed by injecting TGF-β1 into the tunica albuginea.[8] Briefly, rabbits in the TGF-β1 group were anesthetized and were placed on a heating pad to maintain a body temperature of 37°C. After skin disinfection, recombinant human TGF-β1 protein (No. 100-21-10; PeproTech, Rocky Hill, NJ, USA) was injected into the tunica albuginea by a disposable insulin syringe (diameter: 0.33 mm) under ultrasound guidance. The TGF-β1 dose was estimated based on animal weight (dose range: 13–17 μg). The control group did not receive an injection of vehicle. Each injection was introduced into the left side of the mid segment of the dorsal penis. Successful injection was indicated by the formation of a dark liquid area in ultrasound images. An early lesion model was formed within 20 days after the injection of TGF-β1.[9]

Ultrasound examination

Ultrasound examinations were performed by a researcher who was blinded to the experimental grouping. These examinations were performed on the penises of both groups of rabbits before and 20 days after injection using the Aixplorer ultrasound system (SuperSonic Imagine Co., Ltd., Aix-en-Provence, France) with the SL 15-4 probe (SuperSonic Imagine Co., Ltd.). After each rabbit had been anesthetized, the penis was completely exposed for imaging with the transducer in the transverse position, moving at the mid segment of the penis (*i.e.*, injection site). Conventional ultrasound was used to observe the echotexture of the penis and to identify the cord or plaque. 2D-SWE imaging was performed after acquisition of an optimal grayscale image, such that the sample frame was larger than the transverse section of the penis. Elastography images with uniform color were saved in real time. Imaging settings were as follows: the elastography map was scaled from 0 kPa to 50 kPa, while the penetration mode selected for 2D-SWE imaging was "Pen".

For SWQ measurement, the region of interest (ROI) was depicted along the outer boundary of the tunica albuginea surrounding the entire tunica albuginea and cavernosa; the diameter was 2–3 mm, and measurements were performed in kPa. Three representative images with minimal artifacts were chosen for analysis; averages of the "mean" values of SWQ were calculated.

Histological analysis

Histological analysis was performed by a researcher who was blinded to the experimental grouping. Each rabbit was euthanized after ultrasound examination. The penis was separated and fixed in a 4.0% neutral formalin (Sinic Laboratory MEDICINE Technology Co., Ltd., Tongcheng, China), rinsed with water, and then dehydrated with an increasing ethanol gradient (Maixin Bio-Technology Co., Ltd., Shanghai, China). Samples were cleared in xylene (Maixin Bio-Technology Co., Ltd.), then embedded in paraffin (Sinopharm Chemical Reagent Co. Ltd., Shanghai, China), and cut into 3-μm thick sections for subsequent analysis. The staining method and antibody concentrations were identical for specimens from the experimental and control groups.

For hematoxylin–eosin (HE) staining, deparaffinized sections were stained with hematoxylin and eosin (Maixin Bio-Technology Co., Ltd.), followed by dehydration, clearing, and sealing. Sections were observed under a light microscope (Olympus Co., Ltd., Tokyo, Japan) with magnifications of 40× and 200× to analyze penile tissue components.

For sirius red staining, deparaffinized sections were stained with saturated picric acid–sirius red (Maixin Bio-Technology Co., Ltd.), then counterstained with hematoxylin. Following dehydration, clearing, and sealing, the sections were observed under a light microscope (200×) to quantify the proportion of SMCs and CFs, and SMCs/CFs ratio was calculated. The sections were observed under a polarized light microscope (200×; Olympus Co., Ltd.) to quantify the proportion of collagen type I (Col I) and collagen type III (Col III). For each section, five fields were randomly selected for measurement and the mean values were calculated.

For immunohistochemistry, deparaffinized sections were subjected to antigen retrieval in a sodium citrate solution (Maixin Bio-Technology Co., Ltd.) at 98°C. The sections were then treated with 3% hydrogen peroxide solution (Maixin Bio-Technology Co., Ltd.) at room temperature to block endogenous peroxidase activity. Next, the sections were incubated overnight at 4°C with primary antibodies, then incubated at room temperature with appropriate secondary antibodies. Finally, the sections were treated with the 3'3-diaminobenzidine (Maixin Bio-Technology Co., Ltd.) and counterstained with hematoxylin, then dehydrated, cleared, and sealed. Primary antibodies were anti-TGF-β1 antibody (1:50; No. Ab190503; Abcam, Cambridge, UK), antifibronectin antibody (1:50; No. NBP1-51723; Novus Biologicals, Littleton, CO, USA), and anticollagen III antibody (1:100; No. NBP1-05119SS; Novus Biologicals). For the negative control, the primary antibody was replaced with PBS (Maixin Bio-Technology Co., Ltd.); the remaining steps were unchanged. Sections were observed under a light microscope (200×) to measure the positive area proportion (PAP) of TGF-β1 (PAP_T), fibronectin (PAP_F), and Col III (PAP_C). For each section, five fields were randomly selected for measurement and the mean values were calculated.

The method for calculation of the proportion of cells and collagen was as follows. Each pathological section was magnified in a similar manner. Five fields were randomly selected for each section, using a consistent field area. The proportion of cells and collagen in specific fields were obtained by dividing the positive staining areas of cells or collagen in each field by the area of field. The mean proportion of cells and collagen among the five fields was recorded as the representative proportion of cells and collagen in each section. The SMCs/CFs ratio was obtained by dividing the proportion of SMCs by the proportion of CFs. In this study, fibroblasts, smooth muscle cells, collagens, TGF-β1, and fibronectin were evaluated at the junction of the tunica albuginea and cavernosa. We attempted to ensure a 2:1 area ratio of tunica albuginea to cavernosa in each calculated field. If this area ratio could not be achieved in a single field, it was achieved for the total area ratio of tunica albuginea to cavernosa in all five fields in a single section.

Statistical analyses

Statistical analysis was performed using SPSS Statistics, version 22.0 (IBM Corp., Armonk, NY, USA). All data are shown as mean ± s.d. The paired *t*-test was used for univariate comparisons between two groups when normality and homogeneity of variance assumptions were satisfied; otherwise, the Wilcoxon rank-sum test was used. For within-group comparisons, the paired *t*-test or Wilcoxon rank-sum test was used to compare SWQ values before and after TGF-β1 injection. $P < 0.05$ was considered to indicate statistical significance.

RESULTS

In the TGF-β1 group, rabbits were euthanized immediately after ultrasound examination at 20 days after injection of TGF-β1. Rabbits in the control group were also euthanized on that day.

Ultrasound examination results

Conventional ultrasound showed no evidence of penile cord, plaque, or calcification in either group of rabbits, before or after TGF-β1 injection.

2D-SWE images showed that the sample frame was filled with uniform color without artifacts. Before TGF-β1 injection, 2D-SWE image color of the penis was consistent between rabbits in the TGF-β1 and control groups (**Figure 1a** and **1b**). After TGF-β1 injection, image color of the penis differed between rabbits in the TGF-β1 and control groups (**Figure 1c** and **1d**).

Penile SWQ measurements revealed the following findings. Before TGF-β1 injection, penile SWQ values did not significantly differ between the TGF-β1 and control groups (mean ± s.d.: 9.45 ± 1.01 kPa *vs* 9.76 ± 0.86 kPa, $P = 0.470$). After TGF-β1 injection, penile SWQ was significantly greater in the TGF-β1 group than that in the control group (mean ± s.d.: 22.18 ± 1.09 kPa *vs* 9.76 ± 0.56 kPa, $P < 0.001$). In the TGF-β1 group, penile SWQ was significantly greater after TGF-β1 injection than that before TGF-β1 injection (mean ± s.d.: 22.18 ± 1.09 kPa *vs* 9.45 ± 1.01 kPa, $P = 0.005$). In the control group, there was no significant difference in penile SWQ between measurements taken before and after TGF-β1 injection (mean ± s.d.: 9.76 ± 0.86 kPa *vs* 9.76 ± 0.56 kPa, $P = 0.610$), as shown in **Supplementary Table 1**.

HE staining results

HE staining images showed that, compared with the control group, the corpora cavernosa structure in the TGF-β1 group was looser and more disordered; moreover, the normal structure of tunica albuginea between left and right corpora cavernosa was destroyed (**Figure 2a** and **2b**). The numbers of fibroblasts and CFs in penile tissue were greater in the TGF-β1 group than those in the control group (**Figure 2c** and **2d**).

Sirius red staining results

Light microscope images showed that SMCs were stained yellow and CFs were stained red. Yellow areas were significantly less common in the TGF-β1 group than those in the control group; red areas were significantly more common in the TGF-β1 group than those in the control group (**Figure 3**). Light microscope measurements revealed that the proportion of SMCs in penile tissue was significantly lower in the TGF-β1 group than that in the control group (mean ± s.d.: 28.9% ± 7.0% *vs* 41.8% ± 5.6%, $P < 0.001$). However, the proportion of CFs in penile tissue was significantly greater in the TGF-β1 group than that in the control group (mean ± s.d.: 66.8% ± 6.7% *vs* 42.2% ± 4.9%, $P < 0.001$). Additionally, the SMCs/CFs ratio in penile tissue was significantly lower in the TGF-β1 group than that in the control group (mean ± s.d.: 0.45 ± 0.13 *vs* 1.01 ± 0.15, $P < 0.001$), as shown in **Supplementary Table 2**.

Polarized light microscope images showed that Col I appeared red and Col III appeared green. Green areas were significantly more common in the TGF-β1 group than those in the control group; there was no significant difference in red areas between the two groups

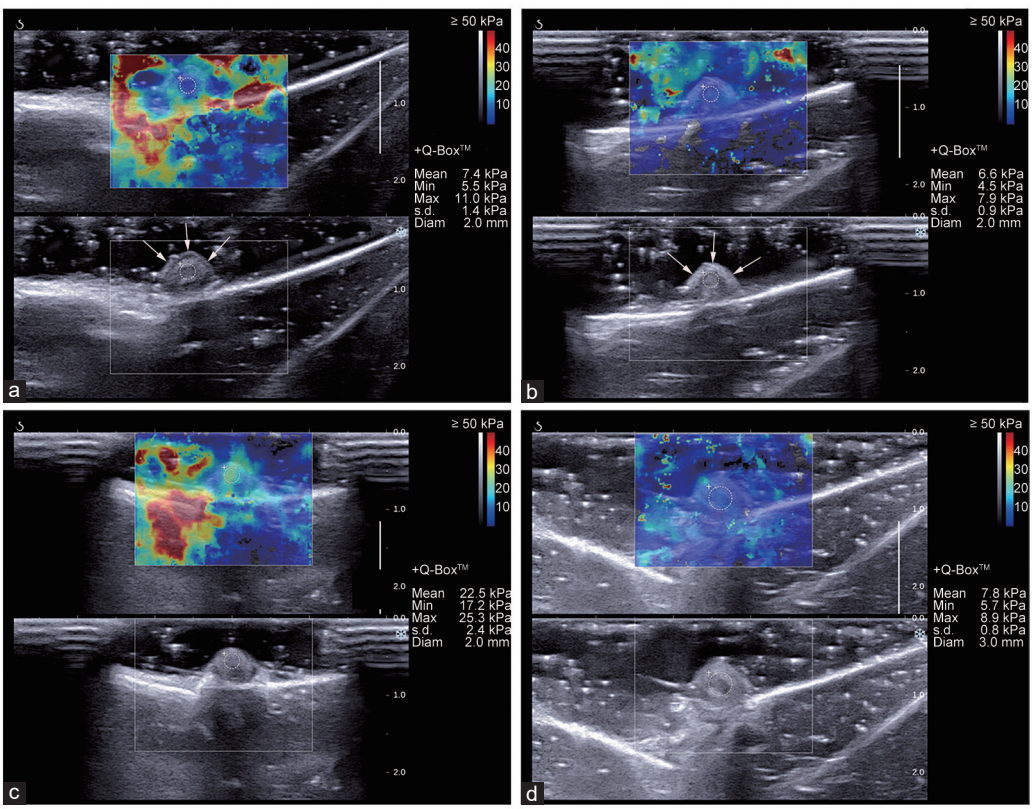

Figure 1: Ultrasound images of rabbit penis. Grayscale images showed no plaque or calcification in the penile tissue in either group before and after TGF-β1 injection. 2D-SWE images showed that: before TGF-β1 injection, the 2D-SWE image colors of rabbit penis were similar between TGF-β1 and control groups; after TGF-β1 injection, the image colors of rabbit penis differed between TGF-β1 and control groups. (**a**) Ultrasound image from a rabbit in the TGF-β1 group euthanized on the day of injection, before TGF-β1 injection. (**b**) Ultrasound image from a rabbit in the control group euthanized on the day of injection, before TGF-β1 injection. (**c**) Ultrasound image from a rabbit in the TGF-β1 group obtained from rabbits euthanized at 20 days after TGF-β1 injection. (**d**) Ultrasound image from a rabbit in the control group euthanized at 20 days after TGF-β1 injection. Q-Box™: measurement results of 2D-SWE; Min: minimum; Max: maximum; s.d.: standard deviation; Diam: diameter; TGF-β1: transforming growth factor β1; 2D-SWE: two-dimensional shear wave elastography. Arrow: skin; circle: tunica albuginea.

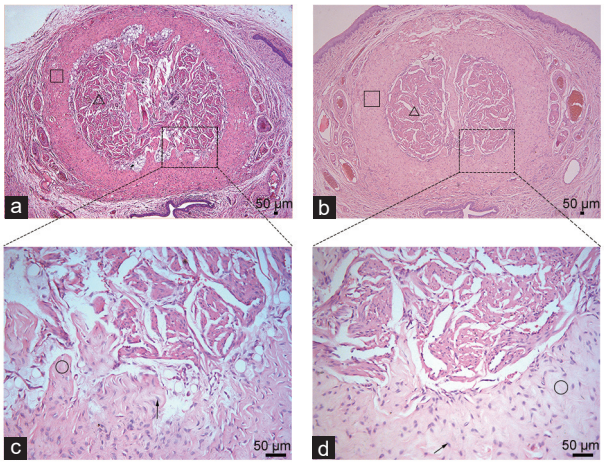

Figure 2: HE staining of penis. The corpora cavernosa structure of TGF-β1 group was looser and more disordered; the normal structure of tunica albuginea between left and right corpora cavernosa was also destroyed. Additionally, the numbers of fibroblasts and collagen fibers in the penis were greater in the TGF-β1 group. (**a**) Image from a rabbit in the TGF-β1 group. (**b**) Image from a rabbit in the control group. (**c**) Image image from a rabbit in the TGF-β1 group. (**d**) Image from a rabbit in the control group. Square: tunica albuginea; triangle: corpora cavernosa; arrow: fibroblasts; circle: collagen fibers. Images were obtained from rabbits euthanized at 20 days after TGF-β1 injection. TGF-β1: transforming growth factor β1; HE: hematoxylin and eosin.

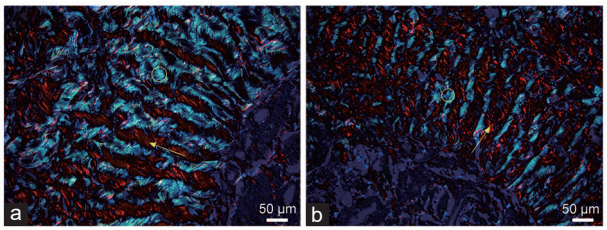

Figure 4: Sirius red staining of penis under a polarized light microscope. Collagen type III staining was more prominent in the TGF-β1 group than in the control group. (**a**) TGF-β1 group; (**b**) control group. Arrow: collagen type I; circle: collagen type III. Images were obtained from rabbits euthanized at 20 days after TGF-β1 injection. TGF-β1: transforming growth factor β1.

(**Figure 4**). Polarized light microscope measurements revealed that the proportion of Col I in penile tissue did not significantly differ between TGF-β1 and control groups (mean ± s.d.: 7.8% ± 7.2% *vs* 7.1% ± 3.1%, $P = 0.529$). However, the proportion of Col III in penile tissue was significantly greater in the TGF-β1 group than that in the control group (mean ± s.d.: 11.9% ± 5.3% *vs* 5.8% ± 1.2%, $P = 0.015$), as shown in **Supplementary Table 3**.

Immunohistochemistry results

Positive areas appeared brown; notably, the positive areas of TGF-β1, fibronectin, and Col III were significantly more common in the TGF-β1 group than those in the control group (**Figure 5**). Immunohistochemistry measurements revealed that PAP_T, PAP_F, and PAP_C in penile tissue were significantly greater in the TGF-β1 group than those in the control group ($P = 0.029$, $P < 0.001$, and $P < 0.001$, respectively; **Supplementary Table 4**).

DISCUSSION

Penile pain, plaque, or malformation during erection and erectile dysfunction are the most common symptoms of CCF. The plaque can usually be detected by palpation and imaging examinations, which are mainly used to evaluate disease progression with proper medical treatment. The most commonly used imaging tools include ultrasound, X-ray, computed tomography (CT), and magnetic resonance imaging (MRI), among which ultrasound is the first choice. Ultrasound is very sensitive to calcifications, and the detection rate of plaques by ultrasound can reach 95%. Nevertheless, X-ray and CT have lower detection rates of noncalcified plaques. MRI also has high sensitivity to plaques, and contrast-enhanced MRI clearly depict inflammatory plaques.[3,10] Overall, regardless of the detection method (*i.e.*, clinical manifestations or imaging examinations), plaque identification is the most important diagnostic basis for CCF. However, the efficacies of conservative and surgical treatments targeting penile plaques remain unclear.[11] Thus far, there is no effective treatment for penile plaques.

Histopathologic changes during CCF are presumably caused by an abnormal wound-healing process. Microtrauma to the penis can

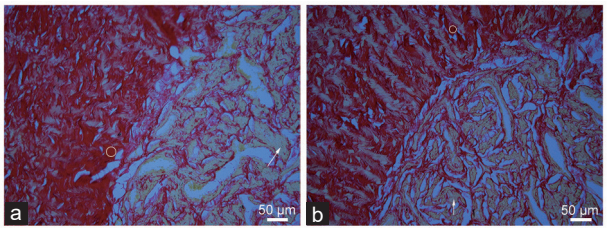

Figure 3: Sirius red staining of penis under a light microscope. There were fewer smooth muscle cells in the TGF-β1 group than in the control group; there were more collagen fibers in the TGF-β1 group than in the control group. (**a**) TGF-β1 group; (**b**) control group. Arrow: smooth muscle cells; circle: collagen fibers. Images were obtained from rabbits euthanized at 20 days after TGF-β1 injection. TGF-β1: transforming growth factor β1.

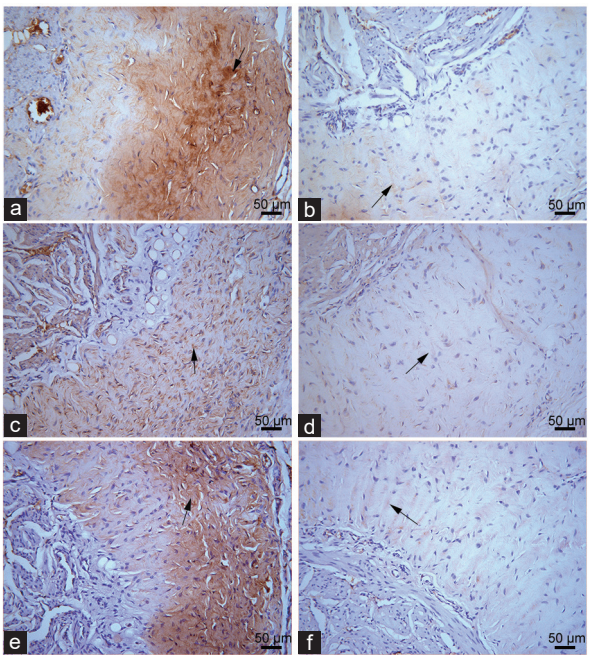

Figure 5: Immunohistochemical staining of penis. Positive areas of TGF-β1, fibronectin, and collagen type III were significantly more prominent in the TGF-β1 group than those in the control group. TGF-β1 in (**a**) TGF-β1 and (**b**) control groups; fibronectin in (**c**) TGF-β1 and (**d**) control groups; collagen type III in (**e**) TGF-β1 and (**f**) control groups. Arrow: positive areas. Images were obtained from rabbits euthanized at 20 days after TGF-β1 injection. TGF-β1: transforming growth factor β1.

cause a small hematoma in the corpora cavernosa, which is followed by fibroblast proliferation, collagen deposition, CFs enhancement, and eventual plaque formation.[1,2,12] Therefore, penile plaque likely occurs in the late stage of CCF development; local tissue components have substantially changed before plaque formation. If the cavernous tissue of the penis is clearly diseased before plaque formation, providing this information to the patient will considerably improve the patient's compliance with preventive medical treatment (*e.g.*, controlling blood pressure, blood sugar, and blood lipids; quitting smoking and drinking; and avoiding excessive and traumatic sexual intercourse). To reduce the risk of penile plaque formation, there is a need to improve the effectiveness of early treatment of CCF.[13–15] Therefore, the early diagnosis of CCF (before plaque formation) is clinically important, although there remains no effective method for this diagnosis.

2D-SWE is a relatively new ultrasound elastography technology, which uses the acoustic radiation force emitted by the probe to induce shear waves that transversely propagate in the tissue. These shear waves are intensified and can be monitored; the SWQ, which reflects tissue stiffness, can be calculated by measuring the shear wave velocity. Tissue stiffness is closely related to histological characteristics, and the tissue stiffness of many lesions (*e.g.*, inflammatory and fibrotic) changes remarkably before morphological changes become visible. Presumably, 2D-SWE can detect abnormal tissue stiffness caused by changes in tissue components before morphological abnormalities, enabling the detection of early lesions. Therefore, if 2D-SWE can successfully detect pathological changes in penile tissue components before plaque formation, it is likely to allow early assessment of CCF.

TGF-β1 can induce increased collagen formation, while inhibiting the activities of collagenase and other proteases; these changes lead to fibrous plaque development.[16–20] Furthermore, exogenous TGF-β1 can induce the expression of endogenous TGF-β1, thereby causing continuous circulation of fibrosis. Fibronectin is a crucial target protein in TGF-β1-induced fibrosis, which can allow static fibroblasts to re-synthesize DNA and secrete large amounts of ECM; these changes can aggravate the degree of fibrosis.[21,22] ECM accumulation negatively affects SMCs, leading to SMCs atrophy and apoptosis. In this study, after the injection of TGF-β1 into rabbit penises, the expression levels of TGF-β1 and fibronectin significantly increased in penile tissue, as did the numbers of fibroblasts and CFs. In contrast, the number of SMCs and the SMCs/CFs ratio significantly decreased. These findings indicated that the fibrosis process had been successfully induced; moreover, the local tissue components of the penis had substantially changed. Cols I and III are the main components of ECM. A large amount of Col III is reportedly present in the immature granulation and scar tissues, whereas the amount of Col I is comparatively lower; subsequently, Col III gradually decreases and Col I increases, thus leading to strengthened tissue intensity.[23,24] The results of this study showed that the content of Col III in rabbit penises was significantly greater in the TGF-β1 group than that in the control group, while there was no significant difference in Col I between the two groups. These findings indicated the presence of early penile lesions.

The ultrasound results of this study showed that no abnormal echo, penile plaque, or calcification was detected by conventional ultrasound after TGF-β1 injection. However, 2D-SWE examination showed that penile SWQ had significantly increased. These findings are consistent with the report by Richard *et al.*[25] who used penile 2D-SWE imaging to examine patients with penile curvature during erection; they found that the tissue location involved in penile curvature was firmer than normal tissue. However, they found no abnormalities by conventional ultrasound or palpation. Our results suggest that 2D-SWE can sensitively identify changes in stiffness that are associated with changes in penile tissue components (*e.g.*, fibroblasts proliferation and CFs accumulation) before the plaque is visible on conventional ultrasound. Thus, 2D-SWE can be used for the early diagnosis of CCF. Additionally, we presume that 2D-SWE can reliably identify corporal fibrosis because 2D-SWE evaluates fibrosis throughout the corpora cavernosa regardless of the location, range, or type of fibrosis (*e.g.*, fibrosis characterized by substantial changes in TGF-β1, Col III, fibronectin, or all three). Furthermore, 2D-SWE has advantages in terms of convenient operation, noninvasiveness, and repeatability; it can also be widely used for follow-up monitoring, localization for treatment, and evaluation of efficacy. Currently, Xiaflex and surgery are the most effective methods for treatment of corpus cavernosum plaque. Plaques are usually allowed to stabilize, then treated with Xiaflex or surgery. However, 2D-SWE can evaluate plaque stiffness because of the close relationship between plaque stiffness and plaque stability. 2D-SWE can significantly improve the accuracy of ultrasonic diagnosis of stabilized plaques; it may thus be more clinically appropriate to diagnose stabilized plaques with 2D-SWE. The clinical value of 2D-SWE in this area merits further analysis.

This study had some limitations. First, the ultrasound examination and histological analysis were performed once after TGF-β1 injection because of the small sample size. The inclusion of additional time points for ultrasound and histological examinations would aid in precise analysis of 2D-SWE sensitivity for detecting early changes in penile components. Second, this study did not include a vehicle-injected control group. Because this study aimed to investigate whether 2D-SWE has greater sensitivity for detecting the onset of penile fibrosis, compared with conventional ultrasound, the injections focused on inducing penile fibrosis; therefore, no vehicle-injected control group was included.

In conclusion, compared with conventional ultrasound, 2D-SWE was superior for identifying changes in stiffness that were associated with fibroblast proliferation and collagen accumulation. Thus, 2D-SWE can be used for the early assessment of CCF.

AUTHOR CONTRIBUTIONS

JFX designed the experiments. LY, JFX, WTR, and JDT acquired the data. JFX, LY, and WTR analyzed and interpreted the data. WTR drafted the manuscript. JFX, LY, and WTR revised the manuscript for intellectual content. All authors read and approved the final manuscript.

COMPETING INTERESTS

All authors declare no competing interests.

ACKNOWLEDGMENTS

This study was supported by grants from the Scientific Research Foundation of Shanghai Pudong Hospital, Fudan University Pudong Medical Center (No. YJRCJJ201804), the Outstanding Clinical Discipline Project of Shanghai Pudong (NO. PWYgy-2018-08), and the Scientific Research Foundation of Shanghai Key Laboratory of Vascular Lesions Regulation and Remodeling (NO. zdsys202008).

Supplementary Information is linked to the online version of the paper on the *Asian Journal of Andrology* website.

REFERENCES

1 Montague DK. New perspectives into Peyronie's disease: etiology, management, and prevention. *Urology* 2019; 125: 6–7.
2 Bilgutay AN, Pastuszak AW. Peyronie's disease: a review of etiology, diagnosis, and management. *Curr Sex Health Rep* 2015; 7: 117–31.
3 Fornara P, Gerbershagen HP. Ultrasound in patients affected with Peyronie's disease. *World J Urol* 2004; 22: 365–7.

4 Nehra A, Alterowitz R, Culkin DJ, Faraday MM, Hakim LS, *et al*. Peyronie's disease: AUA guideline. *J Urol* 2015; 194: 745–53.
5 Zhang X, Zhou B, Miranda AF, Trost LW. A novel non-invasive ultrasound vibro-elastography technique for assessing patients with erectile dysfunction and Peyronie's disease. *Urology* 2018; 116: 99–105.
6 Shiina T, Nightingale KR, Palmeri ML, Hall TJ, Bamber JC, *et al*. WFUMB guidelines and recommendations for clinical use of ultrasound elastography: part 1: basic principles and terminology. *Ultrasound Med Biol* 2015; 41: 1126–47.
7 Bucsics T, Grasl B, Ferlitsch A, Schwabl P, Mandorfer M, *et al*. Point shear wave elastography for non-invasive assessment of liver fibrosis in patients with viral hepatitis. *Ultrasound Med Biol* 2018; 44: 2578–86.
8 Gonzalez-Cadavid NF, Rajfer J. Experimental models of Peyronie's disease. Implications for new therapies. *J Sex Med* 2009; 6: 303–13.
9 El-Sakka AI, Hassoba HM, Chui RM, Bhatnagar RS, Dahiya R, *et al*. An animal model of Peyronie's-like condition associated with an increase of transforming growth factor beta mRNA and protein expression. *J Urol* 1997; 158: 2284–90.
10 Muyshondt C, Faix A, Costa P, Droupy S. Clinical and para-clinical assessment of Peyronie's disease: place of questionnaires and penile duplex ultrasound. *Prog Urol* 2012; 22: 113–9.
11 Serefoglu EC, Hellstrom WJ. Treatment of Peyronie's disease: 2012 update. *Curr Urol Rep* 2011; 12: 444–52.
12 Mulhall JP. Expanding the paradigm for plaque development in Peyronie's disease. *Int J Impot Res* 2003; 15: S93–102.
13 Wan ZH, Li GH, Guo YL, Li WZ, Chen L, *et al*. Amelioration of cavernosal fibrosis and erectile function by lysyl oxidase inhibition in a rat model of cavernous nerve injury. *J Sex Med* 2018; 15: 304–13.
14 Cui K, Tang Z, Li CC, Wang T, Rao K, *et al*. Lipoxin A4 improves erectile dysfunction in rats with type I diabetes by inhibiting oxidative stress and corporal fibrosis. *Asian J Androl* 2018; 20: 166–72.
15 Li WJ, Xu M, Gu M, Zheng DC, Guo J, *et al*. Losartan preserves erectile function by suppression of apoptosis and fibrosis of corpora cavernosa and corporal veno-occlusive dysfunction in diabetic rats. *Cell Physiol Biochem* 2017; 42: 333–45.
16 Hauck EW, Hauptmann A, Schmelz HU, Bein G, Weidner W, *et al*. Prospective analysis of single nucleotide polymorphisms of the transforming growth factor beta-1 gene in Peyronie's disease. *J Urol* 2003; 169: 369–72.
17 Hassoba H, Elsakka A, Lue T. Role of increased transforming growth factor beta protein expression in the pathogenesis of Peyronie's disease. *Egypt J Immunol* 2005; 12: 1–8.
18 Szardening-Kirchner C, Konrad L, Hauck EW, Haag SM, Eickelberg O, *et al*. Upregulation of mRNA expression of MCP-1 by TGF-beta1 in fibroblast cells from Peyronie's disease. *World J Urol* 2009; 27: 123–30.
19 Bivalacqua TJ, Diner EK, Novak TE, Vohra Y, Sikka SC, *et al*. A rat model of Peyronie's disease associated with a decrease in erectile activity and an increase in inducible nitric oxide synthase protein expression. *J Urol* 2000; 163: 1992–8.
20 Chung E, Young LD, Brock GB. Rat as an animal model for Peyronie's disease research: a review of current methods and the peer-reviewed literature. *Int J Impot Res* 2011; 23: 235–41.
21 Quan G, Choi JY, Lee DS, Lee SC. TGF-beta1 up-regulates transglutaminase two and fibronectin in dermal fibroblasts: a possible mechanism for the stabilization of tissue inflammation. *Arch Dermatol Res* 2005; 297: 84–90.
22 Hocking DC, Brennan JR, Raeman CH. A small chimeric fibronectin fragment accelerates dermal wound repair in diabetic mice. *Adv Wound Care* 2016; 5: 495–506.
23 Kataoka T, Kokubu T, Muto T, Mifune Y, Inui A, *et al*. Rotator cuff tear healing process with graft augmentation of fascia lata in a rabbit model. *J Orthop Surg Res* 2018; 13: 200.
24 Hirose K, Kondo S, Choi HR, Mishima S, Iwata H, *et al*. Spontaneous healing process of a supraspinatus tendon tear in rabbits. *Arch Orthop Trauma Surg* 2004; 124: 374–7.
25 Richards G, Goldenberg E, Pek H, Gilbert BR. Penile sonoelastography for the localization of a non-palpable, nonsonographically visualized lesion in a patient with penile curvature from Peyronie's disease. *J Sex Med* 2014; 11: 516–20.

Supplementary Table 1: Penile shear wave elastography quantitative measurements

Group	*Penile SWQ before TGF-β1 injection (kPa)*	*Penile SWQ after TGF-β1 injection (kPa)*	*P*
TGF-β1 group	9.45±1.01	22.18±1.09	0.005
Control group	9.76±0.86	9.76±0.56	0.610
P	0.470	<0.001	

Values are shown as means±s.d. s.d.: standard deviation; SWQ: shear wave elastography quantitative measurement; TGF-β1: transforming growth factor beta 1

Supplementary Table 2: Sirius red staining measurements via light microscopy

Group	*SMCs (%)*	*CFs (%)*	*SMCs/CFs ratio*
TGF-β1 group	28.9±7.0	66.8±6.7	0.45±0.13
Control group	41.8±5.6	42.2±4.9	1.01±0.15
P	<0.001	<0.001	<0.001

Values are shown as means±s.d. SMCs: smooth muscle cells; CFs: collagen fibers; TGF-β1: transforming growth factor beta 1; s.d.: standard deviation

Supplementary Table 3: Sirius red staining measurements via polarized light microscopy

Group	*Col I (%)*	*Col III (%)*
TGF-β1 group	7.8±7.2	11.9±5.3
Control group	7.1±3.1	5.8±1.2
P	0.529	0.015

Values are shown as means±s.d. Col I: collagen type I; Col III: collagen type III; TGF-β1: transforming growth factor beta 1; s.d.: standard deviation

Supplementary Table 4: Immunohistochemistry measurements

Group	*PAP_T (%)*	*PAP_F (%)*	*PAP_C (%)*
TGF-β1 group	30.6±10.8	28.3±5.1	28.0±6.9
Control group	17.6±11.7	15.8±4.4	10.1±6.0
P	0.029	<0.001	<0.001

Values are shown as means±s.d. TGF-β1: transforming growth factor beta 1; PAP_T: positive area proportion of TGF-β1; PAP_F: positive area proportion of fibronectin; PAP_C: positive area proportion of collagen type III; s.d.: standard deviation